



## OPEN The Kv4 potassium channel modulator NS5806 attenuates cardiac hypertrophy in vivo and in vitro

Yue Cai<sup>1,2,3,4,5</sup>, Jiali Zhang<sup>1,2,3</sup>, Hongxue Zhang<sup>1,2,3</sup>, Jinlong Qi<sup>1,2,3</sup>, Chenxia Shi<sup>1,2,3</sup> & Yanfang Xu<sup>1,2,3</sup>✉

The compound NS5806 is a Kv4 channel modulator. This study investigated the chronic effects of NS5806 on cardiac hypertrophy induced by transverse aortic constriction (TAC) in mice in vivo and on neonatal rat ventricular cardiomyocyte hypertrophy induced by endothelin-1 (ET-1) in vitro. Four weeks after TAC, NS5806 was administered by gavage for 4 weeks. Echocardiograms revealed pronounced left ventricular (LV) hypertrophy in TAC-treated mice compared with sham mice. NS5806 attenuated LV hypertrophy, as manifested by the restoration of LV wall thickness and weight and the reversal of contractile dysfunction in TAC-treated mice. NS5806 also blunted the TAC-induced increases in the expression of cardiac hypertrophic and fibrotic genes, including ANP, BNP and TGF- $\beta$ . Electrophysiological recordings revealed a significant prolongation of action potential duration and QT intervals, accompanied by an increase in susceptibility to ventricular arrhythmias in mice with cardiac hypertrophy. However, NS5806 restored these alterations in electrical parameters and thus reduced the incidence of mouse sudden death. Furthermore, NS5806 abrogated the downregulation of the Kv4 protein in the hypertrophic myocardium but did not influence the reduction in Kv4 mRNA expression. In addition, NS5806 suppressed in vitro cardiomyocyte hypertrophy. The results provide novel insight for further ion channel modulator development as a potential treatment option for cardiac hypertrophy.

**Keywords** Cardiac hypertrophy, Kv4 channel, Electrical remodeling, Mouse model, Cardiomyocytes

### Abbreviations

$I_{to}$	Transient outward potassium current
KChIP2	K <sup>+</sup> channel-interacting protein 2
DPP6	Dipeptidyl peptidase-like protein 6
APD	Action potential duration
ET-1	Endothelin-1
QT	QT interval
NRVMs	Neonatal rat ventricular myocytes
TAC	Transverse aortic constriction
VT	Ventricular tachycardia
PVCs	Premature ventricular complexes

Pathological cardiac hypertrophy is a characteristic clinical process in various cardiovascular diseases, including hypertension, myocardial ischemia, and cardiomyopathy<sup>1</sup>. It is characterized by alterations in both cardiac structural and electrical activities and can ultimately result in ventricular dilation and heart failure<sup>2–4</sup>. In addition, the process of cardiac electrical remodeling augments the predisposition to ventricular arrhythmias and thus

<sup>1</sup>Department of Pharmacology, Hebei Medical University, 361 East Zhongshan Road, Shijiazhuang 050017, Hebei, China. <sup>2</sup>The Key Laboratory of New Drug Pharmacology and Toxicology, Hebei Province, Shijiazhuang 050017, China. <sup>3</sup>The Key Laboratory of Neural and Vascular Biology, Ministry of Education, Hebei Medical University, Shijiazhuang 050017, China. <sup>4</sup>Department of Pharmacy, Hebei General Hospital, Shijiazhuang 050051, China. <sup>5</sup>Hebei Key Laboratory of Clinical Pharmacy, Shijiazhuang 050051, China. ✉email: yanfangxu@hebm.u.edu.cn

increases vulnerability to sudden cardiac death (SCD)<sup>5</sup>. The efficacy of available drugs used to prevent heart failure and antiarrhythmic agents is not satisfactory. Most of the drugs for strengthening myocardial contraction have a potential risk of proarrhythmia. Moreover, commonly used antiarrhythmic drugs are likely to induce arrhythmias in hypertrophic and failure hearts. Therefore, there is a great need to develop safe and effective drugs to prevent or reverse structural and electrical remodeling in patients with cardiac hypertrophy.

Calcium-independent transient outward potassium channels carrying the cardiac  $I_{to}$  current are composed of the pore subunits Kv4.2/Kv4.3 and auxiliary subunits. The latter mainly includes potassium channel interacting protein 2 (KChIP2) and dipeptidyl peptidase like protein 6 (DPP6)<sup>6,7</sup>. In rodents, the  $I_{to}$  is the key component of the repolarization stage of the cardiac action potential (AP), and it is responsible for the initial rapid phase of the AP in canines and humans<sup>8,9</sup>. A reduction in the  $I_{to}$  and the resulting lengthening of the action potential duration (APD) are consistent findings in animal models of cardiac hypertrophy and failure as well as human heart failure<sup>10</sup>. Therefore, dysfunction of the  $I_{to}$  is considered to be closely associated with the development of cardiac hypertrophy<sup>11,12</sup>. Several studies have shown that the overexpression of Kv4.3/4.2 or KChIP2 through gene transfer effectively prevents or reverses cardiac hypertrophy in in vivo or in vitro cardiac hypertrophy models<sup>13,14</sup>. Accordingly, upregulation of Kv4 channels is likely a potential strategy for the treatment of cardiac hypertrophy. However, to date, no compounds that intervene in myocardial hypertrophy by enhancing the  $I_{to}$  under pathological conditions have been reported. NS5806 is a small molecule compound and was firstly found to acutely increase the  $I_{to}$  in canine ventricular myocytes isolated from either healthy or failing hearts<sup>15,16</sup>. Whereas, our previous study has demonstrated that NS5806 acutely inhibits native  $I_{to}$  in a concentration-dependent manner in both mouse ventricular cardiomyocytes and human-induced pluripotent stem cell-derived cardiomyocytes (hiPSC-CMs), although it potentiates  $I_{to}$  in the canine ventricular myocytes<sup>17</sup>. Based on the findings, we refer to NS5806 as modulator of Kv4 channels. At present, this Kv4 channel modulator has not yet been tested for its chronic pharmacological effect on the progression of cardiac hypertrophy. In this investigation, we used both in vivo and in vitro models to investigate the chronic effects of NS5806 on cardiac hypertrophy. We first used a pressure overload mouse model for in vivo study since long-term left ventricular pressure overload induced by hypertension is the most common clinical inducer of myocardial hypertrophy. Considering that multiple stimuli including sympathetic-adrenal system, renin-angiotensin system and endothelin etc. contribute to pathological process of cardiac hypertrophy, we further observed its effect in neonatal rat ventricular myocytes (NRVMs) stimulated with endothelin-1 (ET-1) in vitro to clarify whether NS5806 acts directly on cardiomyocytes. The results provide new insight for the therapeutic management of cardiac hypertrophy.

## Materials and methods

### Animal model of cardiac hypertrophy and In Vivo NS5806 administration

Male C57BL/6 mice (weighing 18–22 g, aged 7–8 weeks) were obtained from Vital River Laboratory Animal Technology Co., Ltd. (Beijing, China). All mice were maintained in a controlled environment with a 12 h light/dark cycle, a constant temperature (20–25 °C) and constant humidity (50–60%).

The cardiac hypertrophy mouse model was induced by pressure overload through transverse aortic constriction (TAC) as described previously<sup>18</sup>. In brief, the mice were anesthetized with 1–2% isoflurane in an induction chamber and kept heart rate 450–550 beats per minute. The left second intercostal space was incised for the subsequent operation. The transverse aorta between the innominate artery and left carotid artery was isolated and constricted with a 6–0 silk suture ligature tied against a 26-gauge needle. The needle was swiftly removed to produce a 0.45 mm wide TAC. Mice in the sham-operated group were only exposed to the aorta without ligation. At 4 weeks after TAC surgery, pressure overload-induced cardiac hypertrophy was confirmed to be successfully established by echocardiography, and then the mice were treated with NS5806 (250 mg/kg) or vehicle (0.5% sodium carboxymethyl cellulose) by gavage once a day for 4 continuous weeks. Sham-operated mice received the same dose of NS5806 or vehicle as TAC-treated mice.

### Echocardiography

Mice were anesthetized with 1–2% isoflurane, and cardiac function was monitored via transthoracic two-dimensional (2D)-guided M-mode echocardiography using a Vevo® 2100 system (VisualSonics Inc., Toronto, Canada). The following parameters were subsequently measured: percentage of left ventricular ejection fraction (LVEF) and fractional shortening (LVFS); LV anterior wall dimensions at both diastole and systole (LVAWd and LVAWs, respectively); and LV posterior wall dimensions at both diastole and systole (LVPWd and LVPWs, respectively).

### Electrocardiograph (ECG) recordings

Animal surface ECG recordings were obtained from mice anesthetized with isoflurane (1–2%). Lead II waveforms were acquired by using the BIOPAC/MP150 System (BiopacSystems Inc., USA) at a sampling frequency of 5 kHz. The ECG parameters were manually measured over a period of at least 10 consecutive cardiac cycles during data acquisition in a blinded manner. Heart rate was defined by RR intervals, and the QT interval was the time measured from the beginning of the QRS complex to the end of the T wave.

To determine susceptibility to ventricular arrhythmia, ex vivo ECG recordings were used. The Langendorff-perfused hearts were prepared as previously described<sup>17</sup>. In brief, the hearts were quickly removed, placed on a Langendorff perfusion apparatus and retrogradely perfused with oxygenated Tyrode's solution warmed to 37 °C using a peristaltic pump at a flow velocity of 2–2.5 ml/min. Tyrode's solution containing 140 mM NaCl, 5.4 mM KCl, 2 mM CaCl<sub>2</sub>, 1 mM MgCl<sub>2</sub>, 10 mM HEPES, and 10 mM glucose was adjusted to pH 7.4 with NaOH. Two silver electrodes were attached to the ventricular apex and the aortic root to record lead II equivalent ECGs.

Before conducting the test, the hearts were placed in the thermostatic chamber and given a minimum of 30 min to ensure stable ECG recordings. A BIOPAC/MP150 system at 5 kHz was used to acquire all the data.

### Isolation of mouse ventricular cardiomyocytes

Single ventricular myocytes were obtained through enzymatic isolation from adult male mouse hearts using a protocol that has been previously described<sup>19</sup>. Briefly, the heart was quickly removed and placed on a Langendorff apparatus. Tyrode's solution free of  $\text{Ca}^{2+}$  was used to conduct retrograde aortic perfusion. After 5 min of perfusion, the heart was digested with Tyrode's solution containing type II collagenase (Worthington, 0.5 mg/mL). Subsequently, the heart was removed from the perfusion apparatus upon reaching a state of softening. The LV free wall was dissected, and single cardiomyocytes were harvested and then immersed in a high- $\text{K}^+$  solution composed of (in mM) KOH 80,  $\text{KH}_2\text{PO}_4$  25, KCl 40,  $\text{MgSO}_4$  3, L-glutamic acid 50, taurine 20, EGTA 0.5, HEPES 10 and glucose 10 (pH 7.4 adjusted with KOH). Patch-clamp recording was performed within 4–8 h postisolation.

### Patch-clamp recordings

Electrophysiological recordings of action potentials (APs) and outward voltage-dependent  $\text{K}^+$  currents were performed with an EPC 10 amplifier (HEKA Electronics, Lambrecht, Germany) at room temperature (22–25 °C) under the whole-cell patch-clamp configuration, as previously described<sup>20</sup>. Briefly, for AP recordings, patch pipettes were backfilled with amphotericin (200 µg/ml) to form a perforated patch. The pipette solution consisted of the following ingredients (in mM): 120 mM K-glutamate, 25 mM KCl, 1 mM  $\text{MgCl}_2$ , 1 mM  $\text{CaCl}_2$ , and 10 mM HEPES (pH 7.4 with KOH). The external solution contained (in mM) 4 mM KCl, 138 mM NaCl, 2 mM  $\text{CaCl}_2$ , 1 mM  $\text{MgCl}_2$ , 0.33 mM  $\text{NaH}_2\text{PO}_4$ , 10 mM glucose, and 10 mM HEPES (pH 7.4 with NaOH). APs were evoked in current-clamp mode by using a brief (4–6 ms) current pulse (1 nA) supplied through patch electrodes at a rate of 1 Hz. The APD was measured at 20%, 50% and 90% repolarization ( $\text{APD}_{20}$ ,  $\text{APD}_{50}$  and  $\text{APD}_{90}$ , respectively). Cells with resting potentials above -65 mV were excluded from the study. For outward voltage-dependent  $\text{K}^+$  current recordings, the external solution contained 130 mM N-methyl-D-glucamine (NMG), 5 mM KCl, 1 mM  $\text{MgCl}_2$ , 1 mM  $\text{CaCl}_2$ , 10 mM HEPES, and 10 mM glucose (pH 7.4 with HCl), and the pipette solution contained 140 mM KCl, 4 mM Mg-ATP, 1 mM  $\text{MgCl}_2$ , 10 mM EGTA, and 10 mM HEPES (pH 7.4 with KOH). Nimodipine (1 µM) was added to the external solution to block  $I_{\text{Ca-L}}$ . To isolate distinct  $\text{K}^+$  current components, a rapidly activating and inactivating current,  $I_{\text{to}}$ ; a rapidly activating but slowly inactivating current,  $I_{\text{k,slow}}$ ; and a slowly activating noninactivating current,  $I_{\text{ss}}$ , the decay phases of the currents evoked during long (4.5 s) depolarizing voltage steps to various test potentials were fitted by the sum of two exponentials. The following equation was used:  $y(t) = A1 \cdot \exp(-t/\tau1) + A2 \cdot \exp(-t/\tau2) + A_{\text{ss}}$ , where  $t$  is time;  $\tau1$  and  $\tau2$  are the time constants of decay of  $I_{\text{to}}$  and  $I_{\text{k,slow}}$ , respectively;  $A1$  and  $A2$  are the amplitudes of  $I_{\text{to}}$  and  $I_{\text{k,slow}}$ , respectively; and  $A_{\text{ss}}$  is the amplitude of  $I_{\text{ss}}$ <sup>17</sup>.

### Cell culture and treatments

NRVMs were isolated from 1- to 2-day-old Sprague–Dawley rats (purchased from Vital River Laboratory Animal Technology Co., Ltd., Beijing, China). Hearts were rapidly excised after dislocation of the cervical spine and immediately placed in cold PBS. The ventricles were separated from the atria, and the cells were isolated by enzymatic digestion with 0.125% trypsin–EDTA in PBS at 37 °C. Fetal bovine serum (FBS) was added to the separated cells, which were digested before centrifugation at 1000 rpm for 5 min to collect the pellets. The collected cells were resuspended in Dulbecco's modified Eagle's medium (DMEM) and Ham F12 (1:1 v/v) supplemented with 10% FBS and 1% penicillin–streptomycin and then preplated for 1.5–2 h at 37 °C to allow fibroblasts to adhere to the plate. The unadhered cells were pelleted again and resuspended in DMEM containing 10% FBS, 1% penicillin–streptomycin and bromodeoxyuridine (1:100, to inhibit fibroblast growth). Ventricular myocytes were plated on 6-well plates at a density of  $7.0 \times 10^5$  per well for mRNA experiments. For cell fluorescence staining,  $1.0 \times 10^5$  myocytes per well were plated on 24-well plates. To induce cardiomyocyte hypertrophy, NRVMs were treated with 100 nM ET-1 (Tocris) for 48 h after 24 h of serum starvation in the absence or presence of NS5806 (1 to 10 µM). To measure the cell surface area (CSA), NRVMs were stained with the F-actin marker phalloidin (Sigma) and the nuclear marker Hoechst 33,342 (Sigma). Cell images were captured by using laser confocal microscopy with a 20× objective lens. The CSA of ventricular myocytes was measured by ImageJ software (NIH). CSA was quantified by using the average value of measurements taken from more than 50 randomly selected cells across three independent experiments.

### Quantitative RT–PCR

An Eastep® Super Total RNA Extraction Kit (Promega, USA) was used to extract total RNA. The purity and concentrations of the RNA were quantified by measuring the absorbance at 230, 260 and 280 nm. GoScript™ Reverse Transcription Mix (Promega, USA) (Promega, USA) was used to convert the total RNA (1 µg) to cDNA. The cDNA products were amplified using GoTaq® Green Master Mix (Promega, USA). Each sample was analyzed in triplicate and normalized to GAPDH. The  $2^{-\Delta\Delta\text{CT}}$  method was used to determine the relative expression of the target genes. The primer sequences are listed in Supplemental Table S1.

### Western blot analysis

Fresh or ultralow temperature frozen mouse left ventricular tissue was added to a centrifugation tube, RIPA lysis buffer and the protease inhibitor PMSF (RIPA: PMSF = 100:1, ready to use and mix evenly) were added, and a high-throughput tissue grinder was used to lyse the tissue. After placement and centrifugation, the supernatant (protein sample) was collected. The protein concentrations were determined with a BCA protein assay kit (Pierce, USA). The 40 µg/lane denatured samples were separated by 10% SDS–PAGE before being transferred onto PVDF membranes. Primary antibodies against Kv4.2 (1:500, 75–016, NeuroMab, USA), KChIP2 (1:500, DF14620,

Affinity, China), DPP6 (1:200, APC-146, Alomone, Israel) and GAPDH (1:10,000, 10494-1-AP, Proteintech, China) were incubated at 4 °C overnight. After the membranes were washed with primary antibodies, they were incubated with goat anti-rabbit (611-145-002) or anti-mouse (610-145-121) secondary antibodies (1:5000, Rockland, USA) at room temperature for 2 h. An Odyssey Infrared Imaging System (LICOR 9120; USA) was used to detect the signals.

### Reagents

The chemical name of NS5806 is N-[3,5-Bis(trifluoromethyl)phenyl]-N'-[2,4-dibromo-6-(2H-tetrazol-5-yl)phenyl] urea and its chemical formula is C<sub>16</sub>H<sub>8</sub>Br<sub>2</sub>F<sub>6</sub>N<sub>6</sub>O. The chemical structure of NS5806 is shown in Figure S1. For the in vitro experiments, NS5806 (Tocris, UK) was dissolved in DMSO to prepare a stock solution (20 mM) and stored at -20 °C. For in vivo animal administration, NS5806 was synthesized at the Department of Pharmacology at Hebei Medical University, and its purity was confirmed to be >98% by HPLC (Figure S2, Table S2). A suspension of 0.5% sodium carboxymethyl cellulose (Absin, China) was made with water and stored at -20 °C.

### Statistical analysis

All the experimental data are expressed as the mean ± SEM. GraphPad Prism 7 (GraphPad Software, Inc.) was used to perform the data processing and statistical analysis. Comparisons of data between multiple groups were performed by two-way ANOVA. The nonparametric Kruskal–Wallis test and Dunn's post hoc test were used for the data with a skewed distribution. Fisher's exact tests were used to compare the mortality between groups. When  $P < 0.05$ , the difference was considered statistically significant.

### Ethics

All animal experiments were performed in accordance with the Guide for the Care and Use of Laboratory Animals published by the US National Institutes of Health (NIH Publication, 8th Edition, 2011). The protocol was approved by the Animal Care and Use Committee of Hebei Medical University (approval number: 1604087, Shijiazhuang, China). All methods were carried out in accordance with relevant guidelines and regulations including ARRIVE guidelines.

## Results

### NS5806 alleviated structural remodeling in mice with cardiac hypertrophy in vivo

The effect of in vivo administration of NS5806 on pressure overload-induced mouse cardiac hypertrophy was first examined. Our previous study showed that mouse hearts exhibit robust hypertrophy at the 2nd week after TAC surgery<sup>20</sup>. Accordingly, the treatment began the 4th week after TAC and lasted for another 4 weeks (Fig. 1A). Echocardiograms showed that TAC successfully induced myocardial hypertrophy 4 weeks after surgery (Figure S3). The TAC animals were then assigned to control or NS5806-treated groups. At the end of treatment, echocardiography revealed that a pronounced degree of left ventricular hypertrophy developed in the TAC-treated mice (Fig. 1B). Compared with those in sham mice, left ventricular anterior and posterior wall thicknesses in TAC-treated mice were significantly greater (Fig. 1C,D). There were also significant increases in the heart weight/body weight (HW/BW), heart weight/tibia length (HW/TL) and left ventricular weight/tibia length (LVW/TL) ratios in TAC-treated mice (Figure S4). Moreover, the LVEF and LVFS, which represent cardiac contractile function, were markedly lower in TAC-treated mice than in sham mice (Fig. 1E). These results indicated the successful establishment of cardiac hypertrophy model mice. Administration of NS5806 for four weeks ameliorated these hypertrophic changes, as evidenced by restoring the LV wall thicknesses and weights to the normal values seen in sham mice (Fig. 1B–D, Figure S4) and reversing the dysfunction of cardiac contractile function in TAC-treated mice (Fig. 1E). However, there were no significant alterations of the observed parameters when the sham animals received NS5806.

In addition, a cross-sectional view of the heart showed that TAC induced marked hypertrophy, and the hearts of the NS5806-treated mice displayed a similar appearance to those of the sham mice (Fig. 2A). The expression levels of classic cardiac hypertrophic and fibrotic genes, including atrial natriuretic peptide (ANP), brain natriuretic peptide (BNP), and transforming growth factor- $\beta$  (TGF- $\beta$ ), were markedly increased in TAC-treated mice. However, NS5806 blunted the TAC-induced increase in the expression of these genes (Fig. 2B–D). These data suggested that chronic administration of NS5806 protects against pathological cardiac remodeling.

### NS5806 mitigated electrophysiological remodeling in vivo and ex vivo

We then evaluated the effects of NS5806 on electrical remodeling. In vivo lead II ECG recordings were first performed in mice under isoflurane anesthesia. Representative ECG traces recorded in different animals are shown in Fig. 3A, in which a prolongation of QT intervals was observed in TAC-treated mice. ECG parameters revealed that NS5806 reversed the prolongation of the QT interval in TAC-treated mice, although it had no effect on the QT interval in sham animals (Fig. 3B). There were no significant differences in the RR or PR intervals among the animals (Figure S5). In addition, some TAC-treated mice died without any signs of disease (i.e., sudden death). NS5806 reduced the incidence of sudden death (Fig. 3C). This was likely due to the suppression of malignant ventricular arrhythmias. Therefore, we assessed how NS5806 affects susceptibility to ventricular arrhythmias in isolated hearts through stimulation of beta-receptors by administering the agonist epinephrine. As shown in Fig. 3D, sinus tachycardia was the main manifestation after perfusion of epinephrine in sham mice, while continuous premature ventricular complexes (PVCs), including bigeminy coupled rhythm (upper) and severe ventricular arrhythmias, including ventricular tachycardia (VT) and ventricular fibrillation (VF) (bottom), were exclusively detected in TAC-treated mice. NS5806 markedly decreased the incidence of PVCs and VT/VF

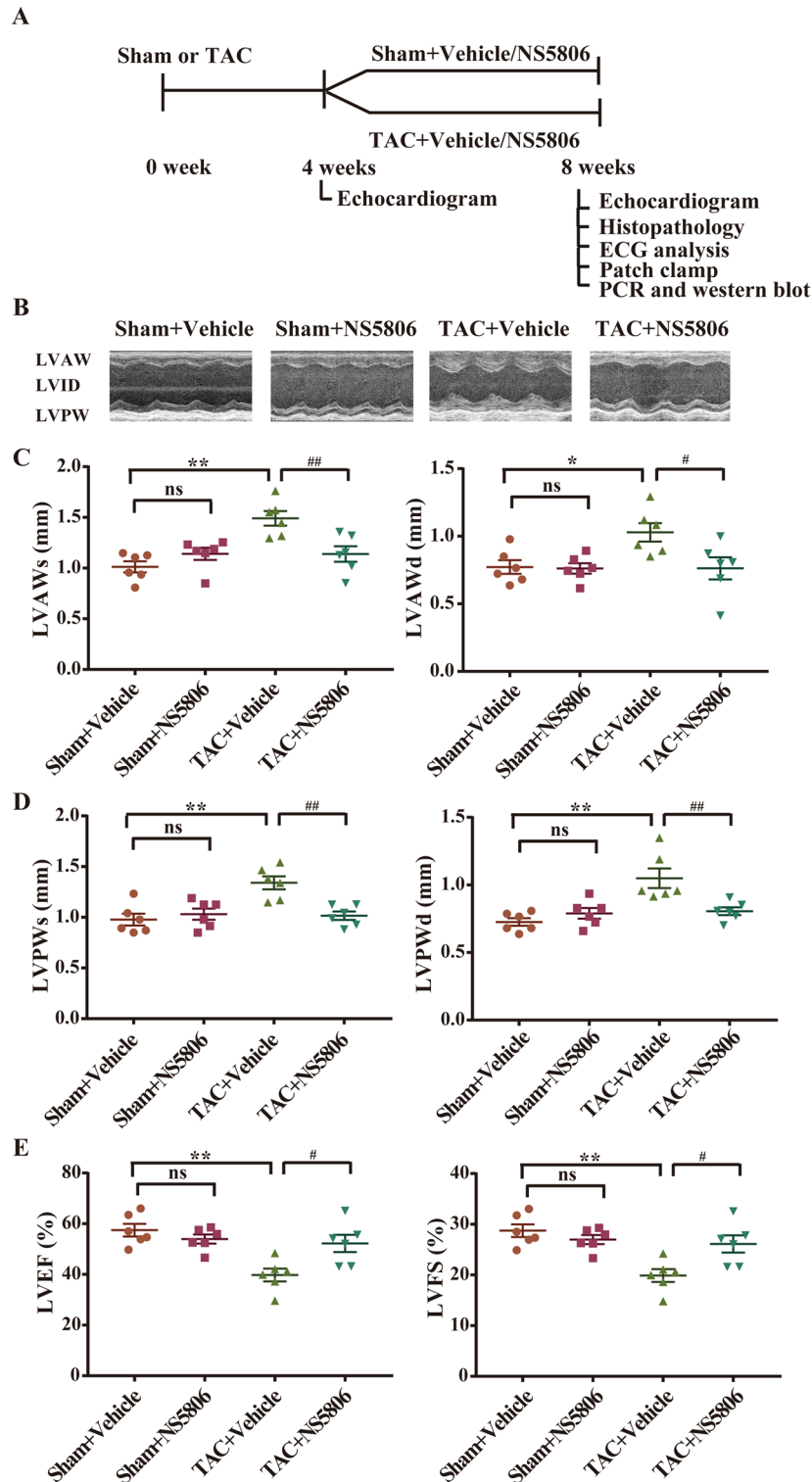


**Fig. 1.** Effects of NS5806 on the wall thickness and function of the left ventricle as determined by echocardiography. **(A)** A schematic diagram of TAC surgery and experimental tests. **(B)** Representative left ventricle M-mode echocardiographic images; **(C–D)** Summary data for the systolic or diastolic left ventricular anterior and posterior wall thickness (LVAWs or LVAWd) (LVPWs or LVPWd); **(E)** Summary data for the left ventricular ejection fraction (LVEF) and fractional shortening (LVFS).  $n = 6$  in each group.  $P < 0.05$ ,  $**P < 0.01$  versus the Sham + Vehicle group.  $\#P < 0.05$ ,  $##P < 0.01$  versus TAC + Vehicle.

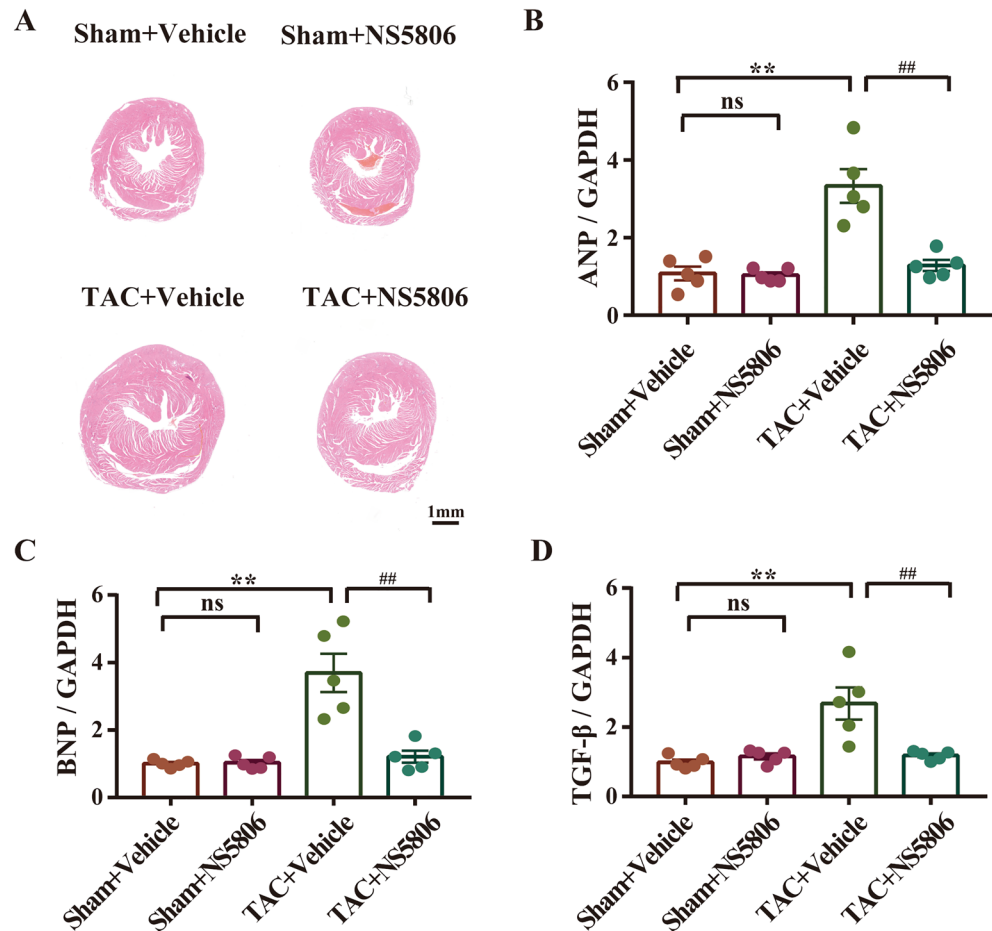


**Fig. 2.** Effects of NS5806 on structural remodeling of the heart. (A) Representative histological images of transverse cardiac sections stained with hematoxylin/eosin; (B–D) Quantification of the mRNA levels of the hypertrophic markers ANP (B) and BNP (C) and the fibrosis marker TGF- $\beta$  (D). GAPDH served as an internal control (n = 5). \* $P < 0.05$ , \*\*  $P < 0.01$  versus the Sham + Vehicle group. # $P < 0.05$ , ## $P < 0.01$  versus TAC + Vehicle.

(Fig. 3E,F). These findings indicated that NS5806 suppressed the vulnerability of TAC-treated mice to VT/VF following catecholamine challenge.

We then investigated the chronic effects of NS5806 on cardiac electrophysiology in isolated mouse ventricular myocytes. Representative AP recordings from different animals are shown in Fig. 4A. The AP repolarization times were 20% (APD<sub>20</sub>), 50% (APD<sub>50</sub>), and 90% (APD<sub>90</sub>), and the AP repolarization times were significantly prolonged in TAC cardiomyocytes, while NS5806 inhibited the prolongation of APD<sub>20</sub>, APD<sub>50</sub> and APD<sub>90</sub> (Fig. 4B). However, NS5806 had no effect on the APD in sham-treated ventricular myocytes. The total outward potassium currents ( $I_K$ ) were evoked using a series of long (4.5 s) depolarizing voltage steps from -50 to +50 mV from a holding potential of -80 mV. Representative current traces among different animals are shown in Fig. 4C, in which TAC myocytes exhibited a visible reduction in peak potassium currents. The peak current densities ( $I_{K,peak}$ ) were calculated, and we found that TAC myocytes had a much lower  $I_{K,peak}$  than sham myocytes at most test potentials, while NS5806-treated mice showed almost normal  $I_{K,peak}$  levels (Fig. 4D). We then differentiated outward currents into  $I_{to}$ ,  $I_{K,slow}$  and  $I_{ss}$  currents by using a double exponential fit to the current decay phases as previously described<sup>21</sup>. At +50 mV, the  $I_{to}$  and  $I_{K,slow}$  densities were significantly decreased in the TAC group although the current amplitudes were similar among different groups (Table S3). NS5806 reversed the TAC-induced reduction of  $I_{to}$  and  $I_{K,slow}$  densities. Similar changes were also observed in  $I_{ss}$  density (Table S3). These findings support the notion that in vivo chronic administration of NS5806 abrogates the decrease in the outward potassium current density and thus attenuates the prolongation of APD and QT intervals in TAC-treated animals.

#### NS5806 alleviated the reduction in Kv4 protein expression in the hypertrophied myocardium

The principal  $\alpha$ -subunit of  $I_{to,f}$  in the mouse heart is considered to be Kv4.2<sup>21,22</sup>. Therefore, we measured the mRNA and protein expression levels of Kv4.2 and the auxiliary subunits KCHIP2 and DPP6. The results showed that the mRNA expression levels of Kv4.2 and KCHIP2 in the TAC group were significantly decreased. NS5806 treatment had no significant effect on the mRNA expression of Kv4.2, KCHIP2 or DPP6 ( $P > 0.05$ ) (Fig. 5A–C). Consistently, the protein expression levels of Kv4.2 and KCHIP2 were reduced in the myocardium of the TAC group, while NS5806 significantly attenuated the reduction in Kv4.2, but did not affect the alteration of KCHIP2

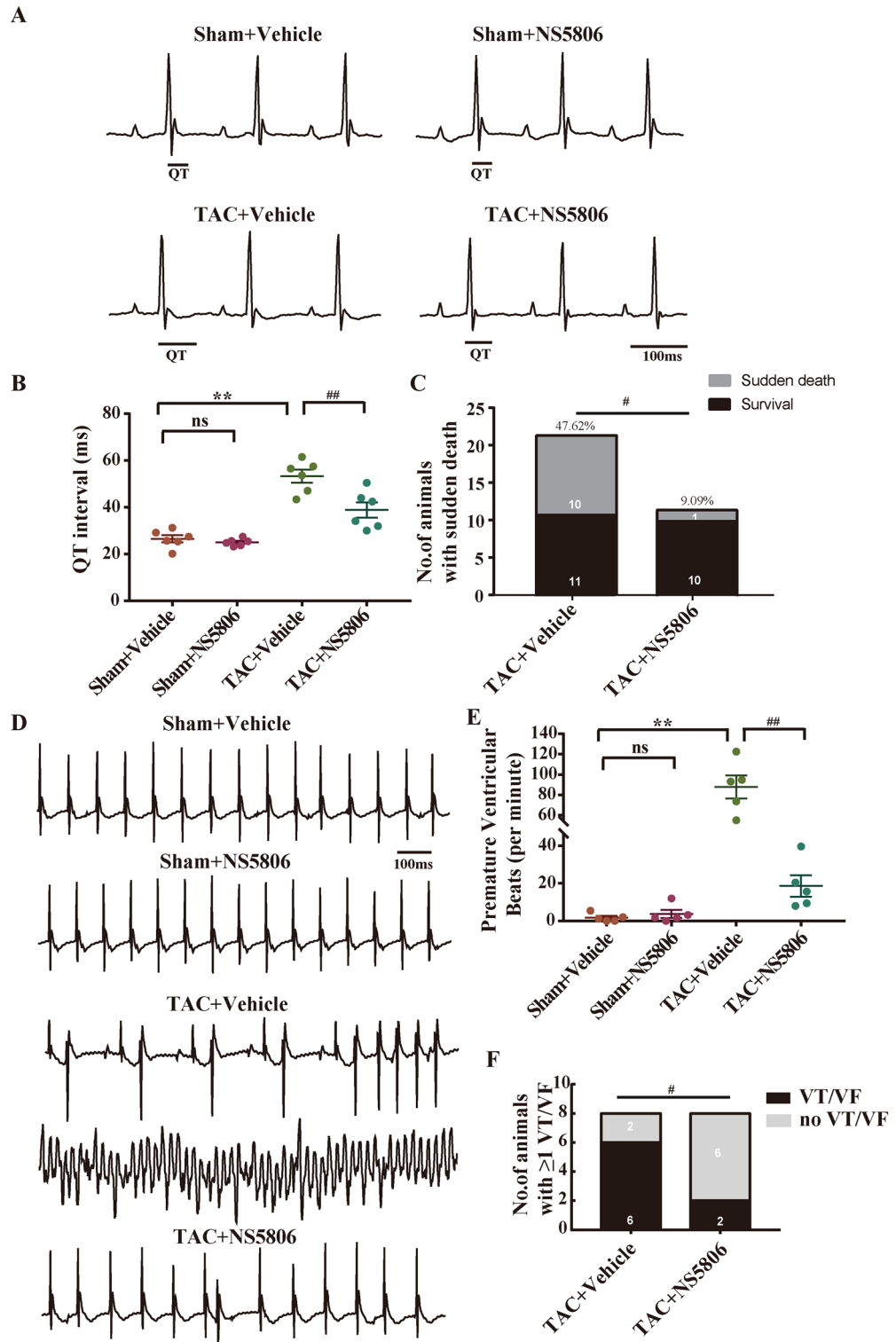


**Fig. 3.** Effects of NS5806 on surface ECG parameters and susceptibility to ventricular arrhythmia. (A) Representative surface ECG traces (lead II); (B) Summary data for QT intervals; n=6 for each group; (C) Summary data for mortality from 4 to 8 weeks after TAC and the statistical analysis was performed with Fisher's exact test; (D) Representative ECG traces of Langendorff hearts perfused with epinephrine; (E) Summary data for PVCs. PVCs were recorded for the first 5 min following the initial PVC, and the data were analyzed as PVCs/min. n=5 for each group; (F) The number of animals with or without VT/VF after epinephrine challenge and the statistical analysis was performed with Fisher's exact test. \* $P < 0.05$ , \*\* $P < 0.01$  versus the Sham + Vehicle group. # $P < 0.05$ , ## $P < 0.01$  versus TAC + Vehicle.

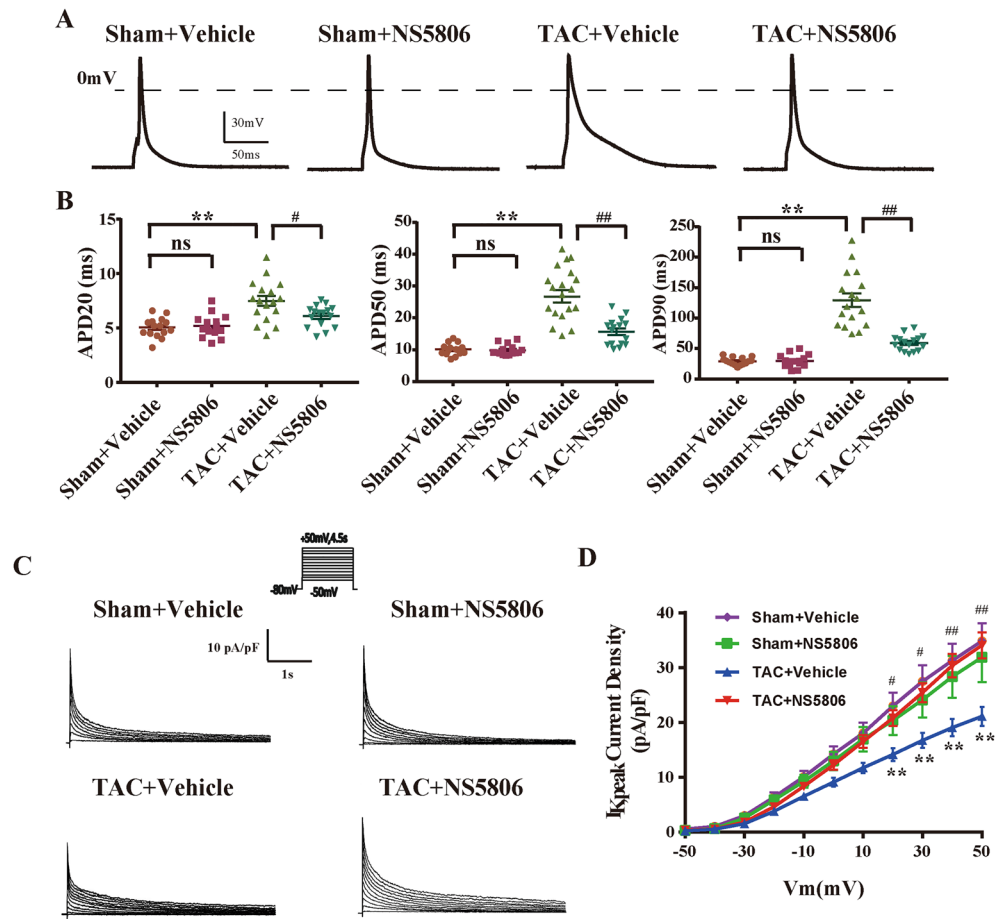


**Fig. 4.** Effects of NS5806 on the left ventricular APD and outward potassium currents of cardiomyocytes. (A) Representative AP traces at 1 Hz stimulation; (B) Summary data for APDs. (C) Representative current traces of the outward potassium currents recorded with the voltage protocol shown in the inset; (D) Average current density–voltage (I–V) relationships of the peak outward currents.  $n \geq 15$  cardiomyocytes from at least 5 mice in each group. \* $P < 0.05$ , \*\* $P < 0.01$  versus the Sham + Vehicle group. # $P < 0.05$ , ### $P < 0.01$  versus TAC + Vehicle.

protein expression ( $P > 0.05$ ) (Fig. 5E–G). These data suggest that NS5806 might suppress the prolongation of APD and QT intervals in hypertrophic hearts by affecting the posttranscriptional processing of the Kv4 protein.

### NS5806 protected against cardiomyocyte hypertrophy in vitro

NRVMs hypertrophy is the most commonly used cell model in vitro. To clarify whether NS5806 acts directly on cardiomyocytes, we further observed the effect of ET-1 on an in vitro cardiomyocyte hypertrophy model in NRVMs<sup>23</sup>. An experimental diagram is shown in Fig. 6A. ET-1 induced visible myocyte hypertrophy and significantly increased the CSA (Fig. 6B,C). NS5806 suppressed the ET-1-induced increase in cell surface area in a concentration-dependent manner (Fig. 6B,C). Consistently, NS5806 inhibited the expression of hypertrophic markers of cardiomyocyte hypertrophy, including ANP, BNP and TGF- $\beta$ , in a concentration-dependent manner (Fig. 6D–F). The in vitro findings revealed a direct beneficial impact of NS5806 on cardiac hypertrophic remodeling.

### Discussion

The findings of the present study mainly include the following: (1) chronic NS5806 administration suppresses pressure overload-induced cardiac hypertrophy in vivo and ET-1-induced cardiomyocyte hypertrophy in vitro; (2) NS5806 alleviates cardiac electrophysiological remodeling in hypertrophic mice, thereby decreasing susceptibility to ventricular arrhythmias; and (3) as a Kv4 channel modulator, NS5806 might protect against pathological cardiac remodeling by increasing the expression of the Kv4 protein.

Our previous study indicated that NS5806 evokes similar acute responses of Kv4 channels in mouse ventricular myocytes and hiPSC-CMs despite species differences in its response<sup>17</sup>. In the present study, we used a pressure overload mouse model for in vivo studies since long-term left ventricular pressure overload induced by hypertension is the most common clinical inducer of myocardial hypertrophy. Our previous observation revealed that the animals generally maintain a normal appearance and activity without an obvious morbid phenotype of



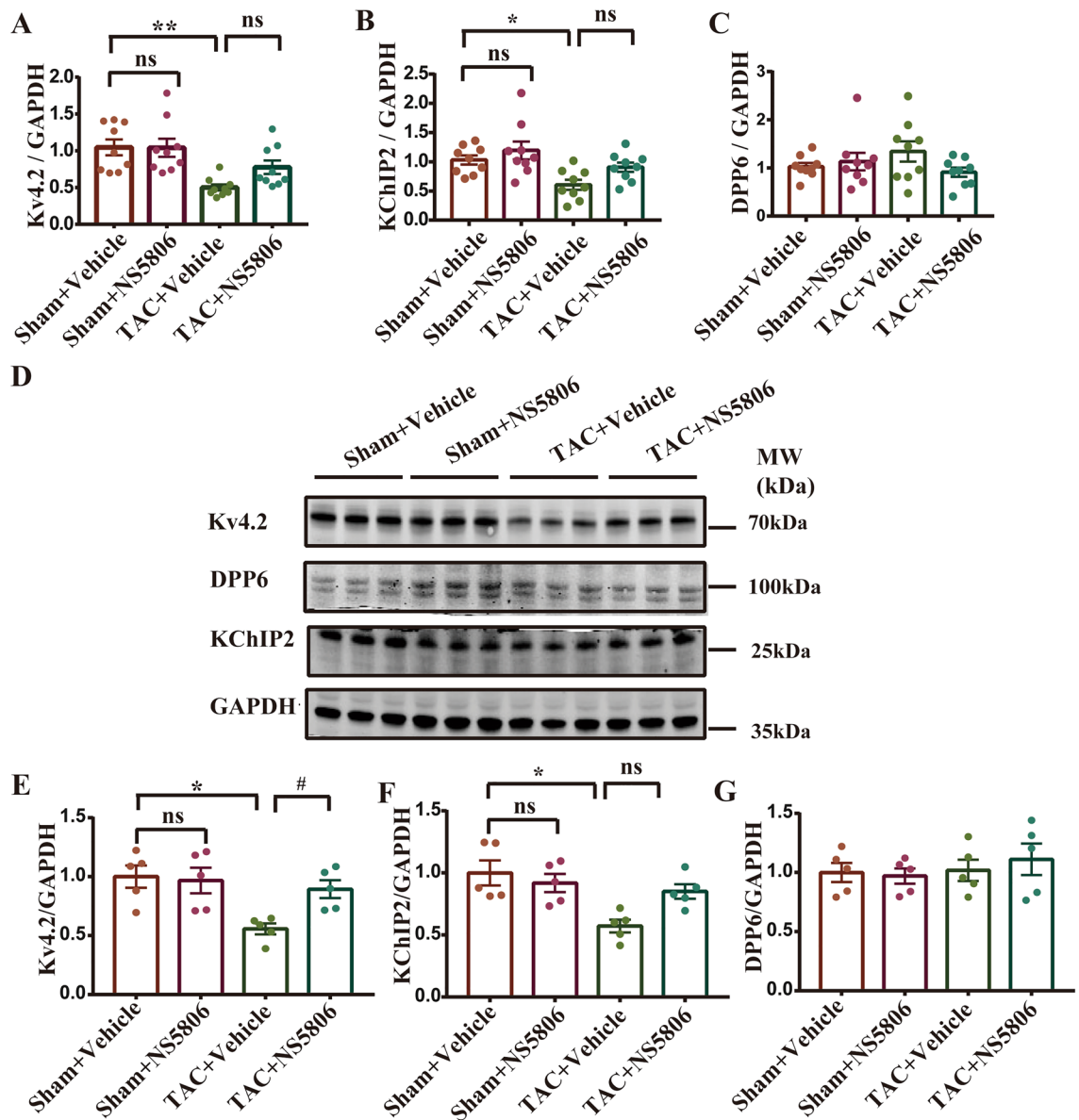


**Fig. 5.** Effects of NS5806 on  $I_{to}$  channel-related gene and protein expression. (A–C) Quantification of the mRNA levels of Kv4.2 (A), KChIP2 (B) and DPP6 (C). GAPDH served as an internal control (n=9 in each group). (D) Representative immunoblots. Original blots are presented in Supplementary Figure S6–7. (E–G) Summary data of Kv4.2 (E), KChIP2 (F) and DPP6 (G) protein levels. GAPDH served as an internal control (n=5 in each group). \* $P < 0.05$ , \*\* $P < 0.01$  versus the Sham + Vehicle group. # $P < 0.05$ , ## $P < 0.01$  versus TAC + Vehicle.

heart failure within 9 weeks after TAC surgery<sup>20</sup>. Accordingly, we treated animals with NS5806 for 4–8 weeks to observe the therapeutic effect of the compound on the hypertrophied heart. No adverse effects were observed with oral doses based on a pilot study. The data indicated that NS5806 significantly attenuated the development of LV hypertrophy in mice after TAC. In addition, our study demonstrated that NS5806 suppressed the development of ET-1-induced cardiomyocyte hypertrophy. The results of the in vitro study provided evidence that NS5806 exerts a direct protective effect against hypertrophic remodeling. In addition, NS5806 restored normal electrical parameters and thus reduced the incidence of sudden death through its suppression of susceptibility to fatal ventricular arrhythmias. However, a previous study showed that a single dose of NS5806 has no effect on increased arrhythmogenicity in heart failure model rats with preserved EF<sup>24</sup>. This discrepancy suggests that the acute pharmacological effect of NS5806 is different from that of chronic administration.

Downregulation of the Kv4 protein occurs in the early stage of cardiac hypertrophy, suggesting the possible involvement of  $I_{to}$  remodeling in the hypertrophic process<sup>25,26</sup>. Therefore, the relationship between cardiac hypertrophy and electrical remodeling has recently become a research hotspot. An early report indicated that downregulation of Kv4.2 through cardiac-specific overexpression of a mutant dominant-negative Kv4.2 causes cardiac hypertrophy and heart failure in mice<sup>27</sup>. The same research group further demonstrated that a reduction

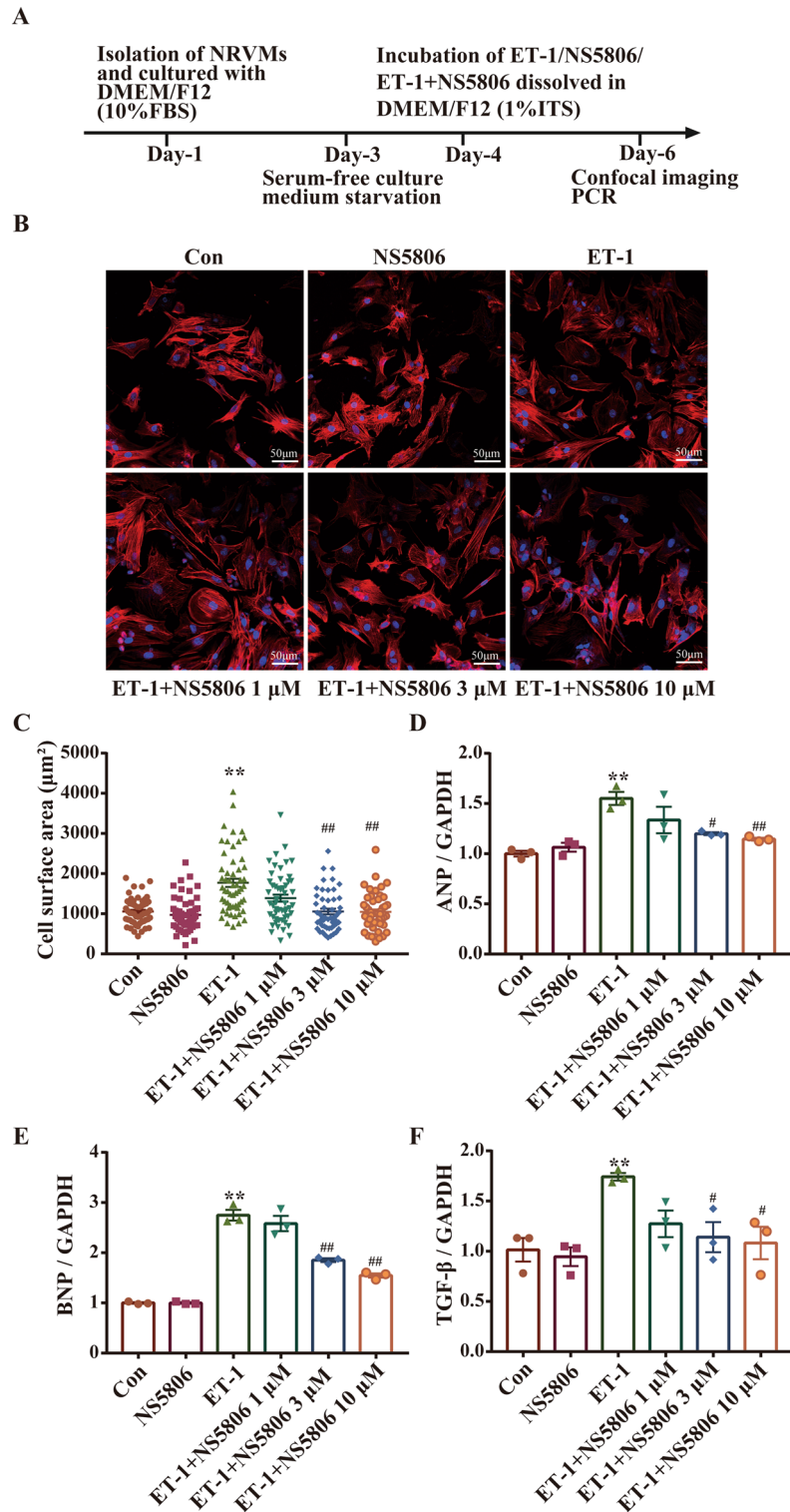


**Fig. 6.** Effects of NS5806 on ET-1-induced hypertrophy in NRVMs. **(A)** A schematic diagram of the experimental tests. **(B)** Representative confocal images of control, NS5806 (3  $\mu$ M) or ET-1 (100 nM), and different concentrations of NS5806 combined with ET-1 for 48 h. The nuclei of the cardiomyocytes were stained with Hoechst (blue), and the intracellular cytoskeleton F-actin was stained with phalloidin (red). **(C)** Quantitative analysis of the CSA of NRVMs ( $n \geq 50$  cells from 3 primary cell preparations in each group). **(D–F)** Quantification of the mRNA levels of the hypertrophic markers ANP, BNP and TGF- $\beta$ . GAPDH served as an internal control. ( $n = 3$  in each group). \* $P < 0.05$ , \*\* $P < 0.01$  versus Con. # $P < 0.05$ , ## $P < 0.01$  versus ET-1.

in the  $I_{to}$  induces cardiomyocyte hypertrophy in NRVMs<sup>28</sup>. Hence, it is postulated that a reduction in the  $I_{to}$  prolongs APD and may cause cardiac hypertrophy<sup>28</sup>. Lebeche et al. demonstrated that in vivo gene transfer of Kv4.3 abrogates the hypertrophic response and rescues the downregulation of the  $I_{to}$  in rats with aortic stenosis<sup>29</sup>. Upregulation of the  $I_{to}$  through overexpression of Kv4.2/4.3 prevents phenylephrine or Ang II-induced cardiomyocyte hypertrophy in cultured NRVMs<sup>13,30</sup>. Moreover, overexpression of KChIP2 in aortic banded adult rats robustly increases  $I_{to}$  densities and significantly attenuates the development of left ventricular hypertrophy<sup>31</sup>. Furthermore, Cao et al. recently demonstrated that the inhibition of miR-27a-3p relieves cardiac hypertrophy and electrical remodeling both in vivo and in vitro by promoting the expression of Kv4.3 at the transcriptional level<sup>32</sup>. The above evidence supports the notion that enhancing the  $I_{to}$  is likely a potential therapeutic approach for preventing/reversing cardiac hypertrophy<sup>33</sup>. However, to date, no compounds have been reported to intervene in myocardial hypertrophy by enhancing the  $I_{to}$  under pathological conditions.

NS5806 was first shown to potentiate the  $I_{to}$  in canine cardiac myocytes by slowing channel decay kinetics<sup>15</sup>. However, a later study revealed that NS5806 increases the ventricular  $I_{to}$  but inhibits the atrial  $I_{to}$  in the rabbit heart, indicating its tissue-dependent pharmacological action<sup>34</sup>. Our recent study showed that in contrast to its promoting effect on the  $I_{to}$  in canine cardiomyocytes, NS5806 evokes an acute inhibitory effect on the mouse ventricular  $I_{to}$  and significantly accelerates the inactivation of the current. Obviously, the acute inhibitory effect of NS5806 on the ventricular  $I_{to}$  in mice does not account for its pharmacological effect under pathological conditions. However, this study has limited information about the molecular mechanism underlying the antihypertrophic effect of NS5806. It is generally accepted that  $I_{to}$  reduction in cardiac hypertrophy is not simply a secondary change, and it may act as a mediator or promoter for pathological development<sup>35</sup>. The reduction of  $I_{to}$  leads to enhanced  $Ca^{2+}$  influx and  $[Ca^{2+}]_i$ , which triggers the activation of hypertrophic gene pathways including calcineurin and calcium-/calmodulin-dependent kinase II (CaMKII). On the other hand, several studies have demonstrated that Kv4 channels on the myocardial cell membrane directly bind to inactive CaMKII protein thereby preventing its activation<sup>36–38</sup>. We found that NS5806 blunted the reduction in the number of Kv4  $\alpha$ -subunits in the hypertrophic ventricular myocardium but had no significant effect on Kv4 mRNA expression. It seems likely that the compound affects the posttranscriptional process of Kv4 channels. The balance between retrograde internalization/degradation from the cell surface and anterograde trafficking determines the amount of functional channels on the cell membrane<sup>39–41</sup>. We speculate that the binding of NS5806 to Kv4 channel complexes may stabilize the channel conformation and thus reduce its degradation as well as the release of CaMKII from cell membrane. In addition, a recent report has shown that NS5806 also acts as an ERK pathway inhibitor to attenuate neuropathic pain<sup>42</sup>. Alternative mechanism beyond Kv4 may also involve in the cardioprotective effect of the compound. Thus, it is interesting to carry out further investigations to elucidate the molecular mechanism underlying the role of NS5806 in cardiac hypertrophy.

In conclusion, our data indicate that compound NS5806 suppresses cardiac hypertrophy in vivo and in vitro. The potential mechanism is likely to involve upregulation of the expression of the Kv4 protein. The findings of this study provide novel insights for the development of new ion channel regulators for the treatment of cardiac hypertrophy.

## Data availability

The datasets used and/or analyzed during the current study are available from the corresponding author upon reasonable request.

Received: 19 January 2024; Accepted: 22 August 2024

Published online: 27 August 2024

## References

- Burchfield, J. S., Xie, M. & Hill, J. A. Pathological ventricular remodeling: mechanisms: Part 1 of 2. *Circulation* **128**, 388–400 (2013).
- Metra, M. & Teerlink, J. R. Heart failure. *Lancet* **390**, 1981–1995 (2017).
- Opie, L. H., Commerford, P. J., Gersh, B. J. & Pfeffer, M. A. Controversies in ventricular remodelling. *Lancet* **367**, 356–367 (2006).
- Drazner, M. H. The progression of hypertensive heart disease. *Circulation* **123**, 327–334 (2011).
- Tomaselli, G. F. & Zipes, D. P. What causes sudden death in heart failure?. *Circ. Res.* **95**, 754–763 (2004).
- Patel, S. P. & Campbell, D. L. Transient outward potassium current, “ $I_{to}$ ”, phenotypes in the mammalian left ventricle: Underlying molecular, cellular and biophysical mechanisms. *J. Physiol.* **569**, 7–39 (2005).
- Niwa, N. & Nerbonne, J. M. Molecular determinants of cardiac transient outward potassium current ( $I_{to}$ ) expression and regulation. *J. Mol. Cell Cardiol.* **48**, 12–25 (2010).
- Clark, R. B., Bouchard, R. A., Salinas-Stefanon, E., Sanchez-Chapula, J. & Giles, W. R. Heterogeneity of action potential waveforms and potassium currents in rat ventricle. *Cardiovasc. Res.* **27**, 1795–1799 (1993).
- Dixon, J. E. et al. Role of the Kv4.3 K<sup>+</sup> channel in ventricular muscle. A molecular correlate for the transient outward current. *Circ. Res.* **79**, 659–668 (1996).
- Näbauer, M. & Kääh, S. Potassium channel down-regulation in heart failure. *Cardiovasc. Res.* **37**, 324–334 (1998).
- Chiamvimonvat, N. et al. Potassium currents in the heart: Functional roles in repolarization, arrhythmia and therapeutics. *J. Physiol.* **595**, 2229–2252 (2017).
- Yang, K. C. & Nerbonne, J. M. Mechanisms contributing to myocardial potassium channel diversity, regulation and remodeling. *Trends Cardiovasc. Med.* **26**, 209–218 (2016).
- Wang, Y., Keskanokwong, T. & Cheng, J. Kv4.3 expression abrogates and reverses norepinephrine-induced myocyte hypertrophy by CaMKII inhibition. *J. Mol. Cell Cardiol.* **126**, 77–85 (2019).
- Liu, W. et al. MG53, a novel regulator of KChIP2 and  $I_{to}$ , plays a critical role in electrophysiological remodeling in cardiac hypertrophy. *Circulation* **139**, 2142–2156 (2019).
- Calloe, K. et al. A transient outward potassium current activator recapitulates the electrocardiographic manifestations of Brugada syndrome. *Cardiovasc. Res.* **81**, 686–694 (2009).
- Cordeiro, J. M. et al. Physiological consequences of transient outward K<sup>+</sup> current activation during heart failure in the canine left ventricle. *J. Mol. Cell. Cardiol.* **52**, 1291–1298 (2012).

17. Zhang, H. *et al.* Auxiliary subunits control biophysical properties and response to compound NS5806 of the Kv4 potassium channel complex. *FASEB J.* **34**, 807–821 (2020).
18. Ding, W. *et al.* Polydatin attenuates cardiac hypertrophy through modulation of cardiac Ca<sup>2+</sup> handling and calcineurin-NFAT signaling pathway. *Am. J. Physiol. -Heart Circ. Physiol.* **307**, H792–H802 (2014).
19. Vander Heide, R. S., Rim, D., Hohl, C. M. & Ganote, C. E. An in vitro model of myocardial ischemia utilizing isolated adult rat myocytes. *J. Mol. Cell. Cardiol.* **22**, 165–181 (1990).
20. Shi, C. *et al.* Temporal alterations and cellular mechanisms of transmural repolarization during progression of mouse cardiac hypertrophy and failure. *Acta Physiol. (Oxf.)* **208**, 95–110 (2013).
21. Xu, H., Guo, W. & Nerbonne, J. M. Four kinetically distinct depolarization-activated K<sup>+</sup> currents in adult mouse ventricular myocytes. *J. Gen. Physiol.* **113**, 661–678 (1999).
22. Liu, J. *et al.* Kv4.3-encoded fast transient outward current is presented in Kv4.2 knockout mouse cardiomyocytes. *PLoS One* **10**, e0133274 (2015).
23. Mueller, E. E. *et al.* Electrical remodelling precedes heart failure in an endothelin-1-induced model of cardiomyopathy. *Cardiovasc. Res.* **89**, 623–633 (2011).
24. Cho, J. H. *et al.* Delayed repolarization underlies ventricular arrhythmias in rats with heart failure and preserved ejection fraction. *Circulation* **136**, 2037–2050 (2017).
25. Wang, Y. & Hill, J. A. Electrophysiological remodeling in heart failure. *J. Mol. Cell. Cardiol.* **48**, 619–632 (2010).
26. Huang, B., Qin, D. & El-Sherif, N. Early down-regulation of K<sup>+</sup> channel genes and currents in the postinfarction heart. *J. Cardiovasc. Electrophysiol.* **11**, 1252–1261 (2000).
27. Wickenden, A. D. *et al.* Targeted expression of a dominant-negative K(v)4.2 K(+) channel subunit in the mouse heart. *Circ. Res.* **85**, 1067–1076 (1999).
28. Kassiri, Z., Zobel, C., Nguyen, T. T., Molkentin, J. D. & Backx, P. H. Reduction of I(to) causes hypertrophy in neonatal rat ventricular myocytes. *Circ. Res.* **90**, 578–585 (2002).
29. Lebeche, D. *et al.* In vivo cardiac gene transfer of Kv4.3 abrogates the hypertrophic response in rats after aortic stenosis. *Circulation* **110**, 3435–3443 (2004).
30. Zobel, C., Kassiri, Z., Nguyen, T. T., Meng, Y. & Backx, P. H. Prevention of hypertrophy by overexpression of Kv4.2 in cultured neonatal cardiomyocytes. *Circulation* **106**, 2385–2391 (2002).
31. Jin, H. *et al.* KChIP2 attenuates cardiac hypertrophy through regulation of Ito and intracellular calcium signaling. *J. Mol. Cell. Cardiol.* **48**, 1169–1179 (2010).
32. Cao, X. *et al.* MiR-27a-3p/Hoxa10 axis regulates angiotensin II-induced cardiomyocyte hypertrophy by targeting Kv4.3 expression. *Front. Pharmacol.* **12**, 680349 (2021).
33. Huo, R., Sheng, Y., Guo, W. T. & Dong, D. L. The potential role of Kv4.3 K<sup>+</sup> channel in heart hypertrophy. *Channels (Austin)* **8**, 203–209 (2014).
34. Cheng, H., Cannell, M. B. & Hancox, J. C. Differential responses of rabbit ventricular and atrial transient outward current (I(to)) to the I(to) modulator NS5806. *Physiological reports* **5**, e13172 (2017).
35. He, Q., Feng, Y. & Wang, Y. Transient outward potassium channel: A heart failure mediator. *Heart Fail. Rev.* **20**, 349–362 (2015).
36. El-Haou, S. *et al.* Kv4 potassium channels form a tripartite complex with the anchoring protein SAP97 and CaMKII in cardiac myocytes. *Circ. Res.* **104**, 758–769 (2009).
37. Alday, A. *et al.* CaMKII modulates the cardiac transient outward K(+) current through its association with Kv4 channels in non-caveolar membrane rafts. *Cell. Physiol. Biochem.* **54**, 27–39 (2020).
38. Keskanokwong, T. *et al.* Dynamic Kv4.3-CaMKII unit in heart: an intrinsic negative regulator for CaMKII activation. *Eur. Heart J.* **32**, 305–315 (2011).
39. Steele, D. F., Eldstrom, J. & Fedida, D. Mechanisms of cardiac potassium channel trafficking. *J. Physiol.* **582**, 17–26 (2007).
40. de Git, K. C., de Boer, T. P., Vos, M. A. & van der Heyden, M. A. Cardiac ion channel trafficking defects and drugs. *Pharmacol. Ther.* **139**, 24–31 (2013).
41. Lamothe, S. M. & Zhang, S. Chapter five-ubiquitination of ion channels and transporters. *Progr. Mol. Boil. Transl. Sci.* **141**, 161–223 (2016).
42. Chiu, C. Y. & Tsaor, M. L. NS5806 inhibits ERK activation to attenuate pain induced by peripheral nerve injury. *Neurosci. Lett.* **790**, 136890 (2022).

### Author contributions

Y.X. designed the experiments and supervised the project. Y.C., J.Z., H.Z., J.Q and C.S. conducted the experiments and contributed to the data analysis. Y.C. prepared the figures. Y.C. and Y.X. wrote the manuscript. All of the authors reviewed and approved the manuscript.

### Funding

This work was supported by the National Natural Science Foundation of China (32071105).

### Competing interests

The authors declare that the research was carried out in the absence of any commercial or financial affiliations that could be seen as potential conflicts of interest.

### Additional information

**Supplementary Information** The online version contains supplementary material available at <https://doi.org/10.1038/s41598-024-70962-x>.

**Correspondence** and requests for materials should be addressed to Y.X.

**Reprints and permissions information** is available at [www.nature.com/reprints](http://www.nature.com/reprints).

**Publisher's note** Springer Nature remains neutral with regard to jurisdictional claims in published maps and institutional affiliations.

**Open Access** This article is licensed under a Creative Commons Attribution-NonCommercial-NoDerivatives 4.0 International License, which permits any non-commercial use, sharing, distribution and reproduction in any medium or format, as long as you give appropriate credit to the original author(s) and the source, provide a link to the Creative Commons licence, and indicate if you modified the licensed material. You do not have permission under this licence to share adapted material derived from this article or parts of it. The images or other third party material in this article are included in the article's Creative Commons licence, unless indicated otherwise in a credit line to the material. If material is not included in the article's Creative Commons licence and your intended use is not permitted by statutory regulation or exceeds the permitted use, you will need to obtain permission directly from the copyright holder. To view a copy of this licence, visit <http://creativecommons.org/licenses/by-nc-nd/4.0/>.

© The Author(s) 2024